Spectroelectrochemical Investigation of Surface States in Nanostructured TiO_2 Electrodes

Gerrit Boschloo* and Donald Fitzmaurice

Department of Chemistry, University College Dublin, Belfield, Dublin 4, Ireland

Received: November 12, 1998; In Final Form: January 12, 1999

Surface states at the nanostructured TiO_2 (anatase)/aqueous electrolyte interface have been investigated using spectroelectrochemical methods. It is found that electrons trapped in these states have an absorption spectrum that differs significantly from that of conduction band electrons. At 400 nm the extinction coefficient of an electron trapped in a surface state is determined to be 1900 M^{-1} cm^{-1}, more than 3 times higher than that of a conduction band electron at the same wavelength. Surface states are located about 0.5 eV below the conduction band edge. Their density is determined to be 3×10^{12} cm^{-2} (microscopic area).

Introduction

Nanoporous nanocrystalline (or nanostructured) semiconductor electrodes have recently been incorporated in several electrochemical systems, such as photoelectrochemical solar cells,[1−12] electrochromic windows,[13−15] and Li-intercalation electrodes.[15−17]

These electrodes have several advantages over conventional single crystalline or polycrystalline semiconductor electrodes. Nanostructured electrodes are composed of small interconnected semiconductor particles (typically 5−50 nm in size). Their internal surface area is 2−3 orders of magnitude larger than their projected surface area and is accessible to the electrolyte solution. As a consequence, it is possible to adsorb a relatively large number of molecules per unit of projected area, a feature which has proved useful in dye-sensitized solar cells[1−7] and electrochromic windows based on redox chromophores.[13,14] The nanostructured geometry also leads to efficient charge separation upon band gap irradiation, as minority carriers only need to travel to a short distance to the semiconductor/electrolyte interface.[8,9] Finally, the nanostructured geometry is advantageous for lithium intercalation electrodes, as lithium ions only have to diffuse a few nanometers in the solid phase.[15−17]

A potential disadvantage of nanostructured electrodes over conventional semiconductor electrodes is the relatively large density of surface states. Surface states are electronic energy levels located at the semiconductor surface. They are involved in electron−hole recombination processes and in electron transfer reactions at the semiconductor/electrolyte interface.[18,19] They are most important when the energies of these states lie in the band gap.

Several studies have reported on the effects of surface states in nanostructured semiconductor electrodes. Specifically, their effects are measured in photocurrent,[3,4,6,11,12] photovoltage,[4,7] charge recombination kinetics,[1,4,20] cyclic voltammetry,[4,16] electrolyte electroreflection,[11] and transient photoconduction.[21] Furthermore, several groups have reported that trapping of electrons in surface states gives an optical response in spectroelectrochemical experiments.[5,10,22−25]

Bedja et al.[5] and Cao et al.[10] attributed the spectra they observed upon negative polarization of nanostructured SnO_2 and TiO_2 electrodes, respectively, to trapped electrons alone. Fitzmaurice and co-workers, however, proposed that the optical response in nanostructured TiO_2 is mainly due to conduction band electrons, with a small contribution of trapped electrons.[22−25]

In a recent study we confirmed that the potential-induced optical changes in nanostructured TiO_2 are mainly due to accumulation of electrons in conduction band states.[26] Using this band filling model, it is possible to explain the observed spectra and to determine the flatband potential.[23] Furthermore, a reasonable value for the effective mass of conduction band electrons in nanostructured anatase can be calculated.[26] At potentials significantly negative of V_{fb}, intercalation of protons and small cations can take place in nanostructured TiO_2, which results in a stronger localization of the accumulated electrons and a significantly different optical response.[15,26]

In this paper it is shown that at applied potentials positive of V_{fb} a small optical response due to trapped electrons can be observed, which is distinctly different from the response of conduction band electrons. Using spectroelectrochemical methods, the density of these trap states is determined, as well as the extinction coefficient of trapped electrons.

Experimental Section

Transparent nanostructured TiO_2 electrodes were prepared as described previously.[2,26] The TiO_2 nanocrystals used to prepare the films consist of pure anatase as determined by XRD. From the line broadening, a particle size of 12 nm is calculated using the Scherrer equation. Films were deposited on F-doped SnO_2 coated glass (TEC 15, Libby Owens Ford, 12 ohm/sq).

The thickness of nanostructured TiO_2 films was measured using a step profiler (Sloan Dektak 3). Reflectance spectra were recorded using a Hewlett-Packard 8452A diode array spectrophotometer with a Labsphere RSA-HP-84 integrating sphere accessory.

Spectroelectrochemical experiments were performed using a glass single-compartment three-electrode cell, with a nanostructured TiO_2 electrode (geometric surface area 1 cm^2) working electrode, a platinum wire counter electrode, and a Ag/AgCl/saturated KCl(aq) reference electrode. The electrolyte, an aqueous solution of 0.2 M $LiClO_4$ buffered with 0.02 M K_2HPO_4/KH_2PO_4 (pH 6.2), was thoroughly deaerated by bubbling with Ar prior to experiments. The cell was incorporated in the sample compartment of a Hewlett-Packard 8452A diode array

* Corresponding author. Present address: Department of Physical Chemistry, Uppsala University, Box 532, 751 21 Uppsala, Sweden.

10.1021/jp984414e CCC: $18.00
Published on Web 03/04/1999

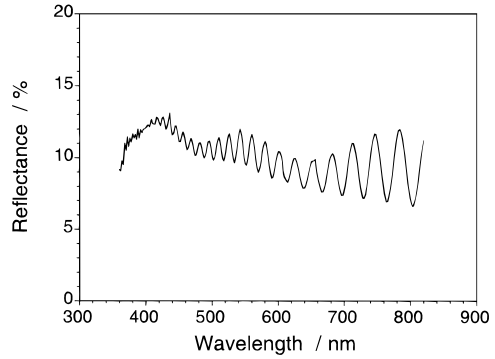

Figure 1. Reflection spectrum (diffuse + specular) of a nanostructured TiO_2 film deposited on SnO_2:F coated glass.

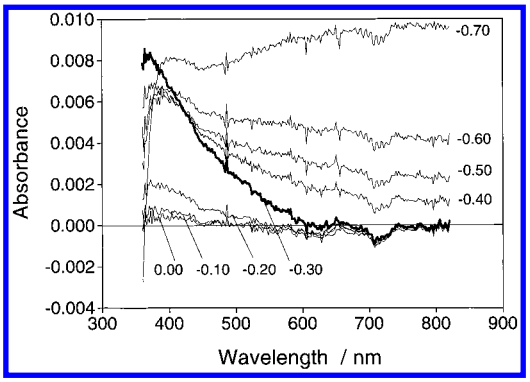

Figure 2. Absorption spectra of nanostructured TiO_2 as function of applied potential. Electrolyte: aqueous $LiClO_4$ (0.2 M), pH 6.2. Spectra are recorded after polarization for 5 min at the indicated potentials. The spectrum measured after stabilization for 15 min at +0.8 V has been subtracted.

spectrophotometer and connected to a Solartron SI 1287 potentiostat. A 360 nm cutoff filter (Schott) was placed in the spectrometer beam to prevent significant direct excitation of the TiO_2. All potentials are reported against Ag/AgCl/saturated KCl (aq).

Results

The UV−vis reflection spectrum of a 4.8 μm thick film of nanostructured TiO_2 (anatase) film on conducting glass is shown in Figure 1. An interference pattern with a short period is observed which is caused by the TiO_2 film. The bare tin oxide substrate gives an interference pattern with a much longer period. The average reflection between 600 and 800 nm, where no absorption by the TiO_2 takes place, is 9.1%, which is slightly lower than that of a bare tin oxide substrate.

Potential-dependent difference spectra of nanostructured TiO_2 at potentials positive of V_{fb} (−0.73 V at pH 6.2[23]) are shown in Figure 2. A very weak but significant and reproducible absorption in the UV−visible region is observed, the absorption being less than 10^{-2} absorbance units. This signal is most clearly observed at −0.30 V. The absorbance is strongest at about 400 nm and decreases gradually to zero at 600 nm. At potentials closer to V_{fb} significant changes in the spectrum occur; i.e., an increase in absorbance is found throughout the visible region, while there is a bleach in the UV region. Experiments performed over a wide pH range (2−12) gave very similar results.

A cyclic voltammogram of a nanostructured TiO_2 electrode is shown in Figure 3a. After 15 min stabilization at +0.80 V, the potential was scanned to −0.80 V, just negative of the flatband potential. A small current peak is observed in the forward scan at −0.38 V. The size of this peak decreases significantly when a second cyclic potential scan is performed directly afterward.

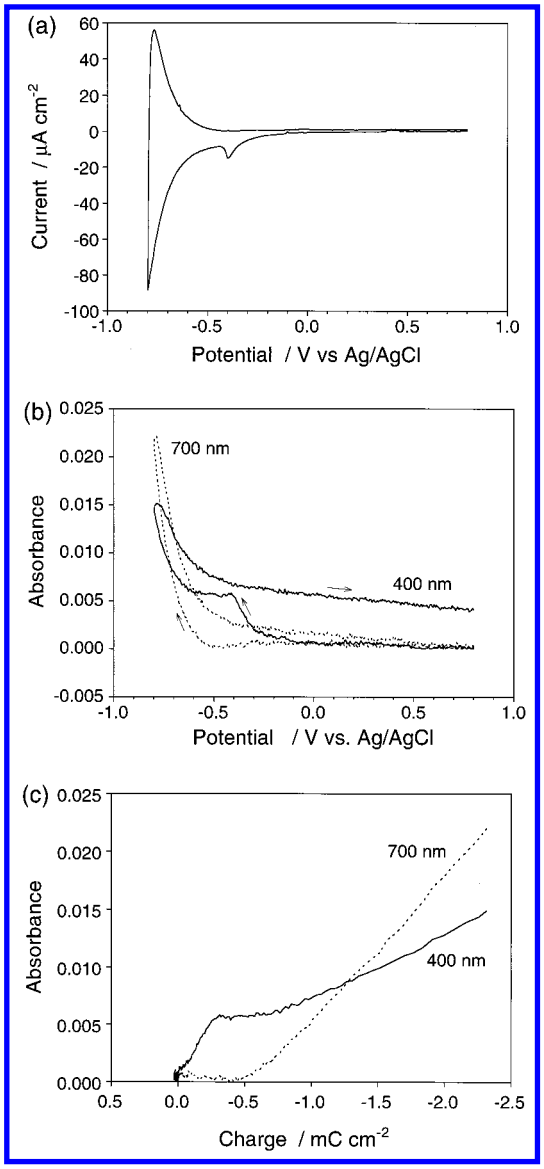

Figure 3. (a) Cyclic voltammogram of a nanostructured TiO_2 electrode in aqueous $LiClO_4$ (0.2 M), pH 6.2. Scan rate 5 mV s^{-1}. (b) Absorbance changes as function of applied potential recorded during (a). (c) Change in absorbance as function of accumulated charge, calculated from the data of (a) and (b).

The changes in absorbance at 400 and 700 nm observed during the potential scan in Figure 3a are shown in Figure 3b. It is clear that during the forward scan the onset of absorbance at 400 nm is at a more positive potential than the onset of absorbance at 700 nm. During the reverse scan the 700 nm absorbance returns to zero, but a considerable residual absorbance is observed at 400 nm. After prolonged polarization at +0.80 V, however, the 400 nm absorption eventually decreases to zero.

In Figure 3c the absorbance (from Figure 3b) is plotted against the charge (calculated from Figure 3a). The behavior of the 400 nm trace is markedly different from the 700 nm trace. Specifically, the initial slope of the 400 nm trace is relatively high (20 cm^2 C^{-1}), whereas that of the 700 nm trace is practically zero. After passing of about 0.4 mC cm^{-2} of cathodic charge, the slope in the 400 nm trace diminishes to 6 cm^2 C^{-1} while the slope of the 700 nm trace increases to 12 cm^2 C^{-1}.

Discussion

The reflectance spectrum of a nanostructured TiO_2 electrode (Figure 1) gives information on the uniformity, the refractive index, the porosity, and the thickness of the film. The strong interference pattern suggests an excellent uniformity of the thickness of the film over the sampled area (about 2 cm^2), which was confirmed by step profiler measurements. From the interference pattern in Figure 1 and the measured thickness of the nanostructured TiO_2 film ($d = 4.8\ \mu m$), the refractive index n_f can be calculated using eq 1:[27]

$$n_f = p\frac{\lambda_1\lambda_2}{2d(\lambda_1 - \lambda_2)} \quad (1)$$

where λ_1 and λ_2 are the wavelengths of two interference maxima and p is the number of maxima between λ_1 and λ_2 plus one. The refractive index is determined to be 1.59 ± 0.03, which is significantly lower than that of bulk anatase ($n_s = 2.52$)[28].

The porosity of the nanostructured TiO_2 film can be determined using a modification of the Lorentz−Lorenz formula (eq 2)[29]

$$\frac{n_f^2 - 1}{n_f^2 + 2} = V_s\frac{n_s^2 - 1}{n_s^2 + 2} \quad (2)$$

where V_s is the volume fraction of solids. Using eq 2, V_s is determined to be 0.53, corresponding to a porosity of 0.47. The above formula assumes a molecular mix of TiO_2 and air ($n_{air} = 1.00$). A perhaps more appropriate and simpler approach is to assume that the refractive index of the nanoporous film is the volume fraction weighed sum of the refractive indices of TiO_2 and air (eq 3):

$$n_f = V_s n_s + (1 - V_s)n_{air} \quad (3)$$

Using this formula, V_s is calculated to be 0.39 and the porosity 0.61. These values are in good agreement with those of Papageorgiou et al., who found 0.36 and 0.64, respectively, for a similar film by using N_2 (BET) adsorption.[29] These values are therefore used in calculations below.

In Figures 2 and 3 a small spectroelectrochemical response is observed in nanostructured TiO_2 at potentials considerably positive of V_{fb}, which is due to trapped electrons. This assignment is made on the basis of the following consideration. Conduction band electrons in nanostructured TiO_2 are not responsible for the observed spectra as the absorption spectrum of these electrons is significantly different from the spectra observed here. Specifically, the absorption spectrum of conduction band electrons is characterized by a bleach at wavelengths shorter than the absorption edge of anatase (384 nm) and a steady increase in absorption at longer wavelengths.[22,23,25,26] A contribution of conduction band electrons can be seen at potentials close to V_{fb} in Figure 2.

Calculations also strongly suggest that the nanostructured TiO_2 film is fully depleted of conduction band electrons at applied potentials positive of V_{fb}. The maximum potential drop ϕ_{sc} in a spherical semiconductor particle under depletion condition is given by eq 4:[31,32]

$$\phi_{sc} = \frac{eN_D}{6\epsilon_r\epsilon_0}r^2 \quad (4)$$

where e is the elementary charge, N_D the donor density, ϵ_r the relative dielectric constant, ϵ_0 the dielectric constant of vacuum, and r the radius of the semiconductor particle. Using the appropriate values for the anatase nanocrystals ($r = 6$ nm and $\epsilon_r = 55$[33,34]), it is found that even for a high donor density of $10^{19}\ cm^{-3}$ the maximum potential drop inside the TiO_2 particle is limited to 20 mV, whereas a negligible 0.2 mV is calculated for $N_D = 10^{17}\ cm^{-3}$, which is a typical value found in undoped anatase thin films.[33,34] A nanostructured film composed of anatase nanocrystals should, therefore, be fully depleted of conduction band electrons at applied potentials positive of V_{fb}.

From the above it is clear that trapped electrons rather than conduction band electrons are responsible for the spectra in Figure 2. The location of the trap states in semiconductor electrodes may be either in the bulk, at grain boundaries, or at the semiconductor /electrolyte interface (i.e., surface states). From Figure 3c it can be deduced that the number of traps in nanostructured TiO_2 corresponds to a charge of about 0.4 mC cm^{-2}, since at this point the trap absorption (monitored at 400 nm) is saturated and the absorption by conduction band electrons (700 nm) starts. As the number of TiO_2 particles per cm^2 (projected area) is about 2.1×10^{14} (calculated using $r = 6$ nm, $d = 4.8\ \mu m$, and $V_s = 0.39$), this corresponds to 12 trapped electrons per particle.

Assuming the trap states to be located in the bulk, the calculated density is $1 \times 10^{19}\ cm^{-3}$. This value appears to be unrealistically high, especially as no evidence is found for the presence of bulk traps in impedance studies of thin dense anatase electrodes.[33,34] Trapping at grain boundaries is a possibility, however, trapping of electrons in surface states is the most likely cause of the observed optical response.

Assuming the trap states to be located at the semiconductor/electrolyte interface, a surface state density of $3 \times 10^{12}\ cm^{-2}$ (microscopic area) is calculated for the nanostructured TiO_2 electrode using the data of Figure 3c (a roughness factor of 770 is assumed, based on a specific surface area of 107 $m^2\ g^{-1}$ [17]). This value seems very reasonable, as it is in excellent accordance with surface state densities found for similar nanostructured TiO_2 electrodes obtained using intensity-modulated photovoltage and photocurrent spectroscopy.[7,12] Specifically, Schlichthörl et al. found an accumulated charge in surface states upon solar irradiation of 200 nC cm^{-2} (microscopic area), corresponding to a surface state density of $10^{12}\ cm^{-2}$ (microscopic area),[7] and de Jongh and Vanmaekelbergh estimated the number of surface states acting as trap to be $10^{12}\ cm^{-2}$ (microscopic area), based on experimentally determined transit and recombination times of photogenerated electrons.[12] Interestingly, a significantly higher density of surface states of $2 \times 10^{13}\ cm^{-2}$ has been found for rutile single crystals using impedance spectroscopy.[35] This electrode, however, was polished and etched, which may have actually increased the density of surface states.[36]

The energetic position of surface states on nanostructured TiO_2 (anatase) is most accurately estimated from the steady-state potentiostatic optical spectra in Figure 2, as there is some delay in the optical response in the potentiodynamic experiment (Figure 3), as will be discussed later. From Figure 2 it can be derived that most surface states are being filled when the potential is changed from −0.20 to −0.30 V. The energetic position of these surface states is therefore about 0.5 eV below the conduction band edge. This value is in excellent agreement with reported values based on transient photocurrent,[6] transient absorption,[24] electrolyte electroreflectance,[11] and charge recombination recombination kinetics[20] of nanostructured TiO_2 (anatase) electrodes. For comparison, surface states in a single crystal

of TiO_2 (rutile) were found to be centered around 0.8 eV below the conduction band edge.[35]

The cyclic voltammogram in Figure 3a was recorded at a slow scan rate of 5 mV/s; however, this was still too fast for the potential to be evenly distributed in the nanostructured TiO_2 film. This becomes clear when the onset of the 400 and 700 nm absorbance at about −0.4 and −0.5 V, respectively, is compared to the onset at these wavelengths in the potentiostatic experiment of Figure 2, where they occur at −0.2 and −0.4 V, respectively. The reason for the slow response to the applied potential in this range is that the nanostructured TiO_2 film is fully depleted of conduction band electrons and therefore insulating. Upon filling of the surface states the nanostructured TiO_2 becomes more conducting.[6,16] The small current maximum in the cyclic voltammogram at −0.38 V (Figure 3a) is due to filling of surface states and the subsequent increase in conductivity.[16]

In course of the reverse scan the absorbance due to trapped electrons decreases only very slowly (Figure 3b). This is probably due to the fact that once the nanocrystals close to the back contact become depleted of electrons, the rest of the film is isolated from the applied potential. Eventually the absorbance decreases to zero due to electron transfer to electrolyte species or slow electron hopping to the back contact.

From Figure 2 it is apparent that the onset of absorption by conduction band electrons occurs at about −0.4 V, that is 0.3 V positive of V_{fb}. This is considerably more positive than is expected on the basis of eq 4. A possible cause is that there is tailing of the conduction band states as suggested by Kay et al.[4]

The slope of the absorption vs charge plot (Figure 3c) corresponds to the coloration efficiency (CE) of the electrode. When it is assumed that no electrons are lost due to electrochemical reaction with solution species, the extinction coefficient of trapped and conduction band electrons in nanostructured TiO_2 can be calculated using $\epsilon = 96.5 \times CE$, where ϵ has the units $M^{-1}\ cm^{-1}$ and CE $cm^2\ C^{-1}$. For trapped electrons ϵ_{400} is found to be 1900 $M^{-1}\ cm^{-1}$, while that for conduction band electrons is about 3 times lower ($\epsilon_{400} = 600\ M^{-1}\ cm^{-1}$). At 700 nm the extinction coefficient for conduction band electrons in nanostructured TiO_2 is calculated to be 1200 $M^{-1}\ cm^{-1}$, which is in good agreement with previously determined values.[4,26]

Conclusions

Electrons trapped in surface states of nanostructured TiO_2 (anatase) can be observed using spectroelectrochemical methods. Their absorption spectrum differs significantly from that of conduction band electrons. Surface states are located about 0.5 eV below the conduction band edge. Their density is determined to be $3 \times 10^{12}\ cm^{-2}$ (microscopic area).

Acknowledgment. We thank Declan Ryan for preparation and X-ray analysis of the colloidal TiO_2. This work was financially supported by the European Union under the Joule III program.

References and Notes

(1) O'Regan, B.; Moser, J.; Anderson, M.; Grätzel, M. *J. Phys. Chem.* **1990**, *94*, 8720.
(2) O'Regan, B.; Grätzel, M. *Nature* **1991**, *353*, 737.
(3) Schwartzburg, K.; Willig, F. *Appl. Phys. Lett.* **1991**, *58*, 2520.
(4) Kay, A.; Humphry-Baker, R.; Grätzel, M. *J. Phys. Chem.* **1994**, *98*, 952.
(5) Bedja, I.; Hotchandani, S.; Kamat, P. V. *J. Phys. Chem.* **1994**, *98*, 4133.
(6) Boschloo, G. K.; Goossens, A. *J. Phys. Chem.* **1996**, *100*, 19489.
(7) Schlichthörl, G.; Huang, S. Y.; Sprague, J.; Frank, A. J. *J. Phys. Chem. B* **1997**, *101*, 8141.
(8) Hodes, G.; Howell, I. D. J.; Peter, L. M. *J. Electrochem. Soc.* **1992**, *139*, 3136.
(9) Hagfeldt, A.; Björksten, U.; Lindquist, S.-E. *Sol. Energy Mater. Sol. Cells* **1992**, *27*, 293.
(10) Cao, F.; Oskam, G.; Searson, P. C.; Siripala, J. M.; Heimer, T. A.; Farzad, F.; Meyer, G. J. *J. Phys. Chem.* **1995**, *99*, 11974.
(11) Boschloo, G. K.; Goossens, A.; Schoonman, J. *J. Electroanal. Chem.* **1997**, *428*, 25.
(12) de Jongh, P. E.; Vanmaekelbergh, D. *J. Phys. Chem. B* **1997**, *101*, 2716.
(13) Marguerettaz, X.; O'Neill, R.; Fitzmaurice, D. *J. Am. Chem. Soc.* **1994**, *116*, 2629.
(14) Cinnsealach, R.; Boschloo, G.; Rao, S. N.; Fitzmaurice, D. *Sol. Energy Mater. Sol. Cells* **1998**, *55*, 215.
(15) Hagfeldt, A.; Vlachopoulos, N.; Grätzel, M. *J. Electrochem. Soc.* **1994**, *141*, L82.
(16) Kavan, L.; Kratochvilová, K.; Grätzel, M. *J. Electroanal. Chem.* **1995**, *394*, 93.
(17) Kavan, L.; Grätzel, M.; Rathousky, J.; Zukal, A. *J. Electrochem. Soc.* **1996**, *143*, 394.
(18) Morrison, S. R. *Electrochemistry at Semiconductor and Oxidised Metal Electrodes*; Plenum Press: New York, 1980.
(19) *Semiconductor Electrodes*; Finklea, H. O., Ed.; Elsevier: Amsterdam, 1988.
(20) Haque, S. A.; Tachibana, Y.; Klug, D. R.; Durrant, J. R. *J. Phys. Chem. B* **1998**, *102*, 1745.
(21) Könenkamp, R.; Henninger, R.; Hoyer, P. *J. Phys. Chem.* **1993**, *97*, 7328.
(22) O'Regan, B.; Fitzmaurice, D.; Grätzel, M. *Chem. Phys. Lett.* **1991**, *183*, 89.
(23) Rothenberger, G.; Fitzmaurice, D.; Grätzel, M. *J. Phys. Chem.* **1992**, *96*, 5983.
(24) Redmond, G.; Grätzel, M.; Fitzmaurice, D. *J. Phys. Chem.* **1993**, *97*, 6951.
(25) Fitzmaurice, D. *Sol. Energy Mater. Sol. Cells* **1994**, *32*, 289.
(26) Boschloo, G.; Fitzmaurice, D. *J. Phys. Chem. B*, submitted for publication.
(27) Chopra, K. L. *Thin Film Phenomena*; McGraw-Hill: NewYork, 1969; p 102.
(28) *Handbook of Chemistry and Physics*, Lite, D. R., Ed.; CRC Press: Boca Raton, FL, 1997.
(29) Born, M.; Wolf, E. *Principles of Optics*; Pergamon Press: Oxford, UK, 1975.
(30) Papageorgiou, N.; Barbé, C.; Grätzel, M. *J. Phys. Chem. B* **1998**, *102*, 4156.
(31) Albery, W. J.; Bartlett, P. N. *J. Electrochem. Soc.* **1984**, *131*, 315.
(32) Goossens, A. *J. Electrochem. Soc.* **1996**, *143*, L131.
(33) Boschloo, G. K.; Goossens, A.; Schoonman, J. *J. Electrochem. Soc.* **1997**, *144*, 1311.
(34) van de Krol, R.; Goossens, A.; Schoonman, J. *J. Electrochem. Soc.* **1997**, *144*, 1723.
(35) Siripala, W.; Tomkiewicz, M. *J. Electrochem. Soc.* **1982**, *129*, 1240.
(36) Miki, T.; Yanagi, H. *Langmuir* **1998**, *14*, 3450.